Supporting Information

Steering two-electron O_2 electroreduction on Co-N-C catalyst via native carbon defect engineering for highly efficient H_2O_2 production

Shuqi Tian, Guanlong Wang*, Xiufang Zhang*

School of Light Industry and Chemical Engineering, Dalian Polytechnic University, Dalian 116034, China.

*Corresponding author: Guanlong Wang; E-mail: wanggl@dlpu.edu.cn

Xiufang Zhang; E-mail: zhangxf@dlpu.edu.cn

Experimental Section

Text S1 Chemicals and materials

Cobalt nitrate hexahydrate, zinc nitrate hexahydrate, 2-methylimidazol, Nafion D-521 dispersion (5 wt.%), methanol, sulfuric acid, sodium sulfate, ferrous sulfate heptahydrat, cerium sulfate, hydrogen peroxide, Carbon fiber paper (CFP) was purchased from Toray, Ultrapure water (Millipore Milli-Q grade) with a resistivity of 18.2 MΩ was used in all the experiments.

Text S2 Characterization

The crystal structure of the D-Co-N-C-X was characterized by X-ray diffraction. The morphologies were observed with a scanning electron microscope (SEM; JSM-6700F, 5 keV). The AC-STEM used is the Japanese JEOL JEM-ARM300F2. The EDS element mapping was carried out in a JEOL ARM-200 microscope at 200 kV. The N_2 adsorption/desorption isotherms were obtained by ASAP 2020, Micromeritics, USA. Specific surface area and pore size distribution were calculated based on Brunauer-Emmett-Teller (BET) Model and density functional theory (DFT). Raman spectra were analyzed using a Renishaw Raman spectrometer by exciting a 514.5 nm Ar-ion laser. Extended X-ray Absorption Fine Structure (EXAFS) is carried out using the Shanghai Synchrotron Radiation Facility. X-ray photoelectron spectroscopy (XPS) was carried out on an AXIS-ULTRA DLD-600W instrument, and the binding energy (BE) was calibrated using the C 1s peak at 284.8 eV. The UV-vis spectroscopy of $Ce(SO_4)_2$ titrant solution and RhB titrant solution were measured on Shimadzu UV-2800S spectrophotometer.

Text S3 Formula

$$E_{RHE} = E_{Ag/AgCl} + 0.1976 + 0.059 \times pH \quad \textbf{(1)}$$

$$H_2O_2\% = \frac{200 \times I_{ring}/N}{|I_{disk}| + I_{ring}/N}$$

(2)

$$n = \frac{4|I_{disk}|}{|I_{disk}| + I_{ring}/N}$$

(3)

$$2Ce^{4+} + H_2O_2 == 2Ce^{3+} + 2H^+ + O_2 \quad \textbf{(4)}$$

$$C_{H_2O_2} = \frac{V_{Ce^{4+}} \times C_{before}Ce^{4+} - (V_{Ce^{4+}} + V_{removedelectrolyte}) \times C_{after}Ce^{4+}}{2 \times V_{removedelectrolyte}}$$

(5)

$$H_2O_2\ production\ rate = \frac{C_{H_2O_2} \times V_{electrolyte}}{m \times t} \quad \textbf{(6)}$$

$$FE(\%) = \frac{C_{H_2O_2} \times V_{electrolyte} \times 2 \times F}{\int_0^t idt}$$

(7)

$V_{Ce^{4+}}$: The volume of Ce^{4+} initially added, $C_{before}Ce^{4+}$: The concentration of Ce^{4+} initially introduced, $V_{removedelectrolyte}$: Volume of the electrolyte solution taken after the reaction, $C_{after}Ce^{4+}$: Volume of Ce^{4+} after Reaction, $V_{electrolyte}$: Referring to the total volume of the electrolyte solution, m: Mass of the catalyst used, t: Reaction Time, F: Faraday's constant, 96485 C/mol

Text S4 DFT method

All the DFT calculations were conducted based on the Vienna Ab initio Simulation Package (VASP).[1,2] The exchange-correlation potential was described by the Perdew−Burke−Ernzerhof (PBE) generalized gradient approach (GGA).[3] The electron-ion interactions were accounted by the projector augmented wave (PAW).[4] All DFT calculations were performed with a cut-off energy of 400 eV, and the 2×2×1 Gamma centered Monkhorst-Pack grids k-points were selected to sample the Brillouin zone integration. The energy and force convergence criteria of the self-consistent iteration were set to 10^{-5} eV and 0.03 eV $Å^{-1}$, respectively. DFT-D3 method was used to describe van der Waals (vdW) interactions.[5]

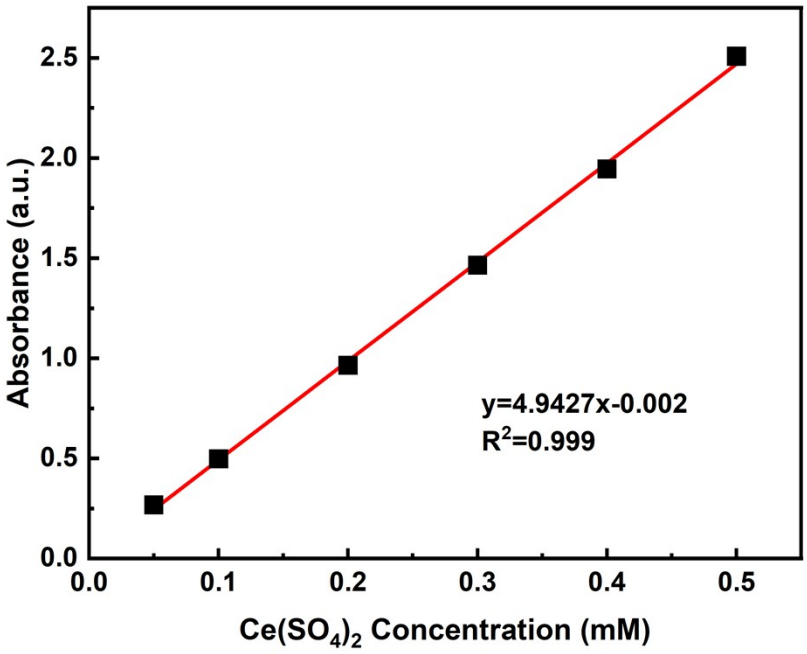

Fig. S1 The standard curve of $Ce(SO_4)_2$ solution

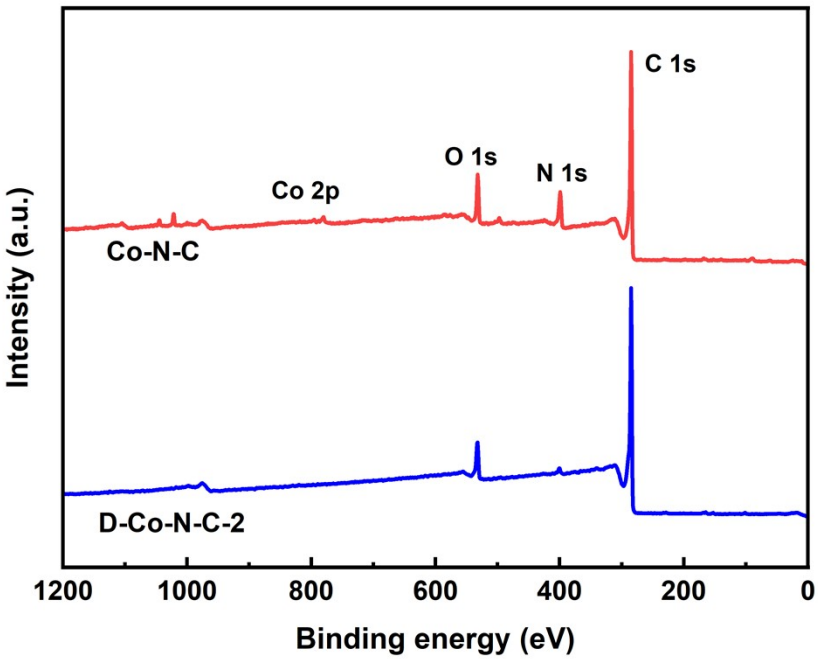

Fig. S2 XPS spectra of Co-N-C and D-Co-N-C-2

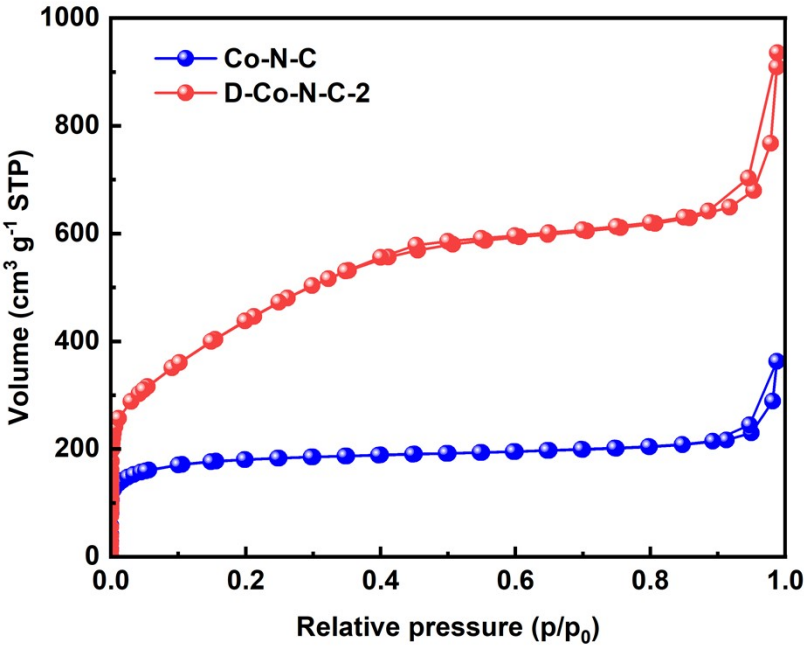

Fig. S3 N_2 adsorption-desorption isotherms of Co-N-C and D-Co-N-C-2.

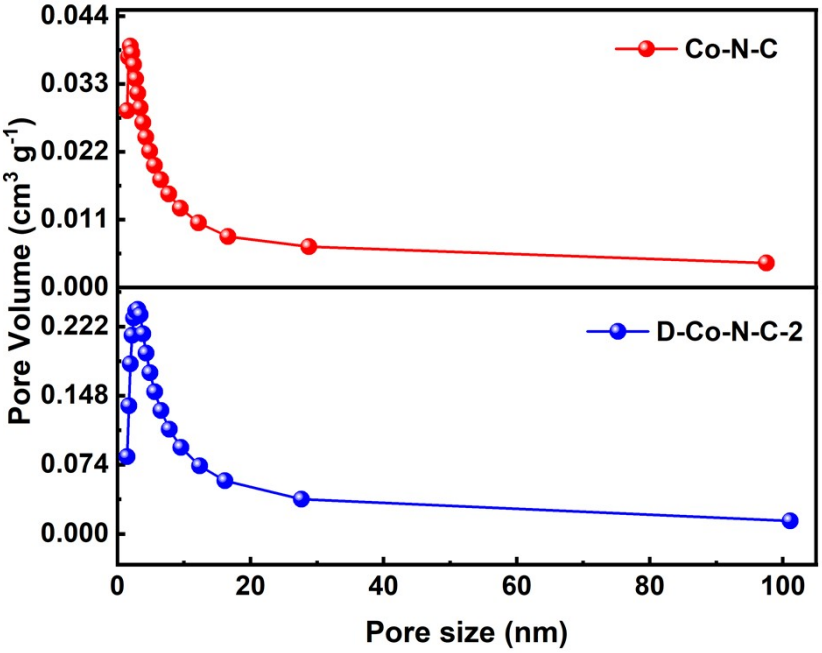

Fig. S4 The pore size distribution curves of Co-N-C and D-Co-N-C-2.

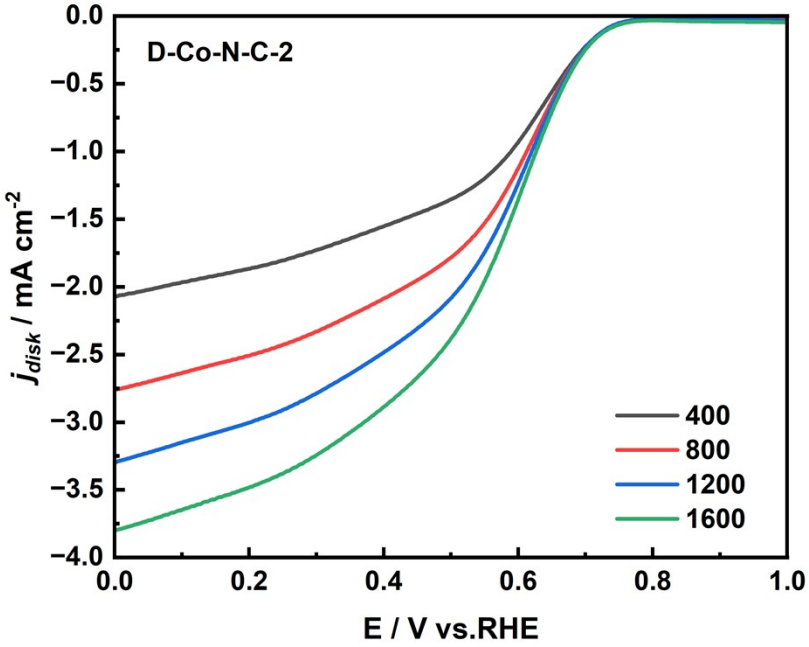

Fig. S5 RRDE polarization curves of D-Co-N-C-2 at different rotational speeds.

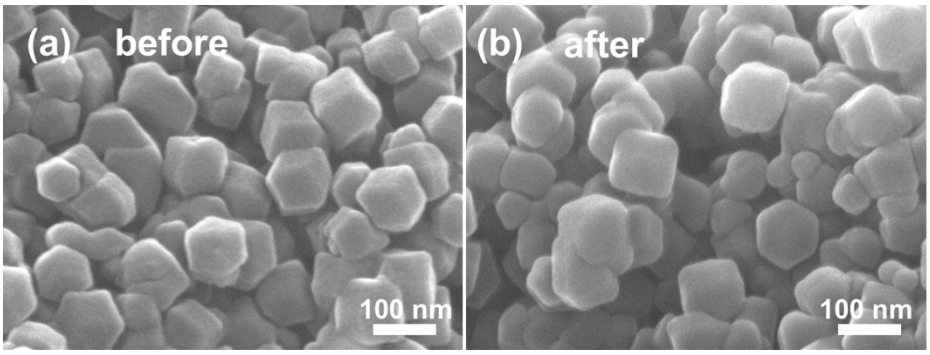

Fig. S6 SEM images of D-Co-N-C-2 (a) before long-term operation, (b) after long-term operation.

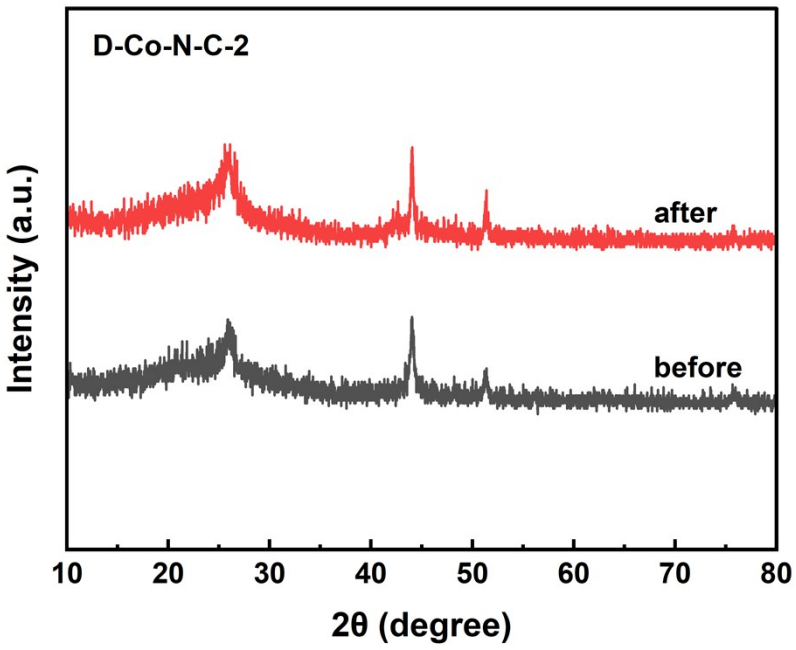

Fig. S7 XRD patterns of Co-N/P-C-0.75 before and after long-term operation.

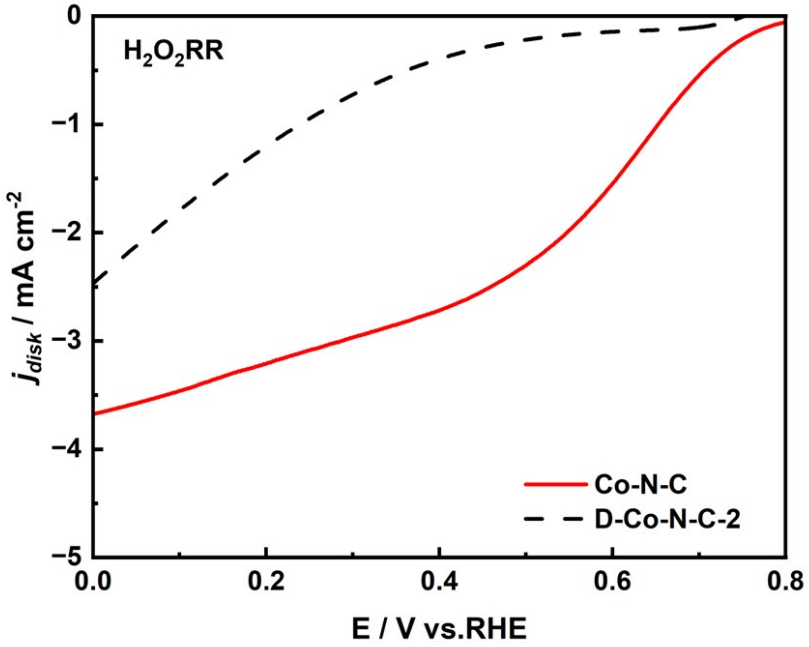

Fig. S8 the H_2O_2RR polarization curve of D-Co-N-C-2 and Co-N-C.

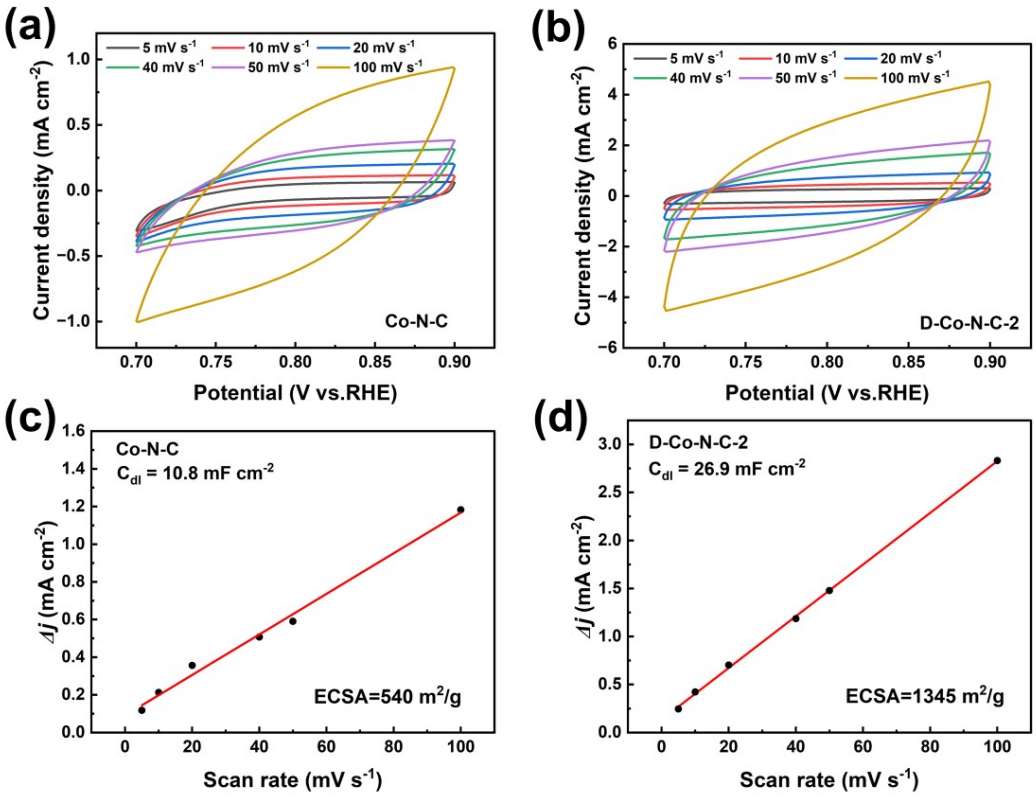

Fig. S9 Cyclic voltammograms (CVs) of (a) Co-N-C and (b) D-Co-N-C-2 in 0.05 M H_2SO_4 saturated with N_2 at different scan rates (5-100 mV s^{-1}); the corresponding double-layer capacitance values of (c) Co-N-C and (d) D-Co-N-C-2.

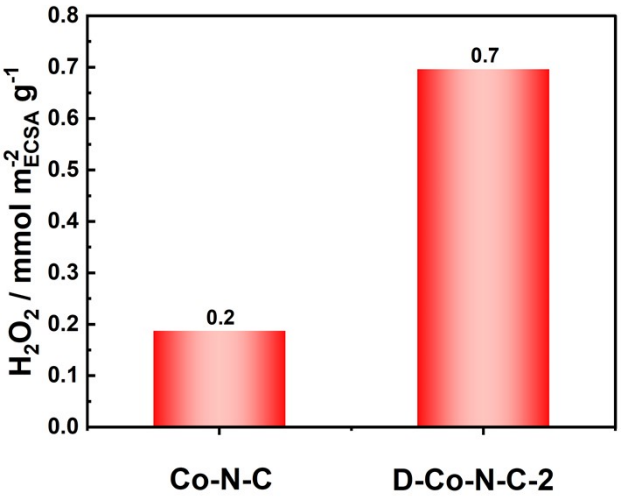

Fig. S10 The H_2O_2 production rate per unit electrochemical active area of Co-N-C and D-Co-N-C-2.

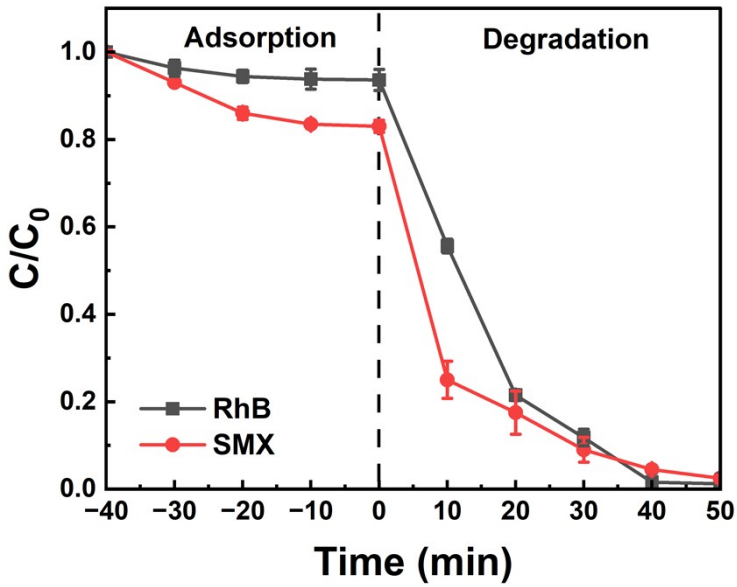

Fig. S11 The removal of RhB in the electrolyte and SMX in surface water by D-Co-N-C-2 in the electro-Fenton system.

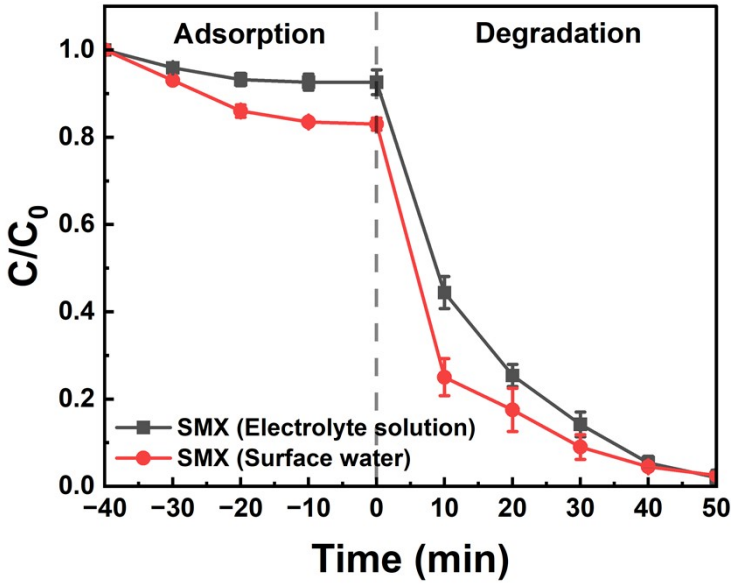

Fig. S12 The removal of SMX in the electrolyte and surface water by D-Co-N-C-2 in the electro-Fenton system.

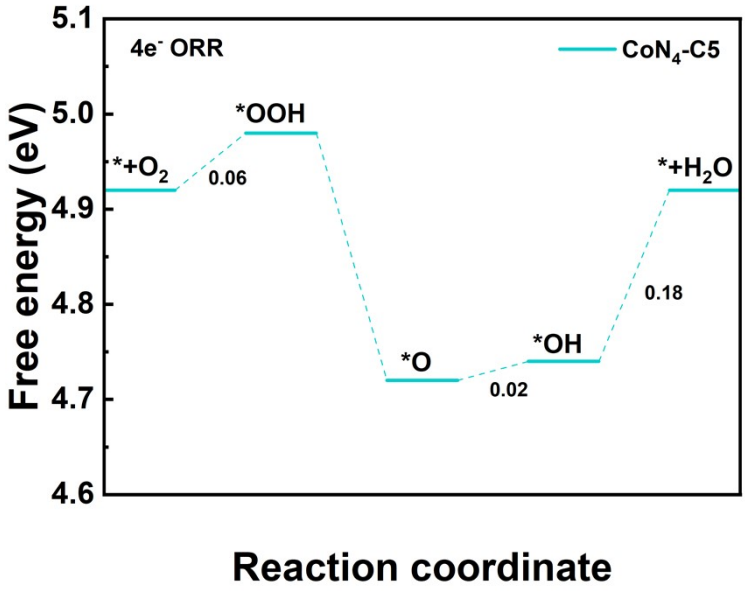

Fig. S13 Free energy diagrams for the $4e^-$ ORR pathway in Co-N_4-C5 systems at equilibrium potential.

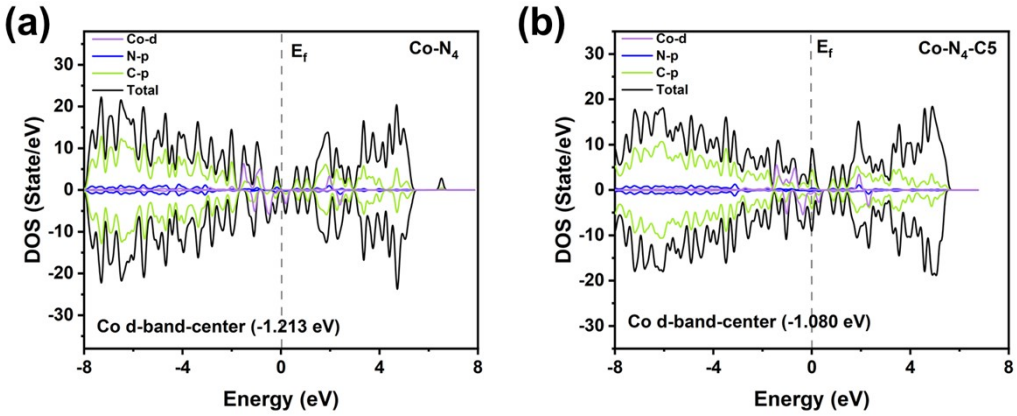

Fig. S14 (a) (b) The PDOS diagrams of Co-N-C and D-Co-N-C-2.

Table S1 EXAFS fitting parameters at the Co K-edge for various samples（S_0^2=0.70from Co-foil）

	shell	CN[a]	R[b](Å)	σ^{2c}(Å^2)	ΔE_0[d](eV)	R factor
Co-foil	Co-Co	12*	2.48±0.01	0.0062	6.3±0.5	0.001
CoO	Co-O	6*	2.09±0.04	0.0137	2.9±1.0	0.006
	Co-Co	12*	3.00±0.02	0.0102		
Co2O3	Co-O	6*	2.02±0.09	0.0089	2.4±1.2	0.017
	Co-Co	12*	2.99±0.03	0.0048		
Co3O4	Co-O	4*	1.99±0.04	0.0056	7.9±1.9	0.017
	Co-Co	6*	2.96±0.01	0.0094		
	Co-Co	6*	3.47±0.01	0.0069		
CoPc	Co-N	4*	1.97±0.02	0.0079	7.0±1.3	0.011
D-Co-N-C-2	Co-N	3.73±0.3	1.96±0.04	0.0052	-3.9±0.3	0.005
	Co-Co	6.76±0.2	2.49±0.01	0.0048		

[a]*CN*: coordination numbers; [b]*R*: bond distance; [c]σ^2: Debye-Waller factors; [d] ΔE_0: the inner potential correction. R factor: goodness of fit. Error bounds that characterize the structural parameters obtained by EXAFS spectroscopy were estimated as CN±20%; R ± 1%; σ^2 ± 20%.

Table S2 The Bader charge of Co-N_4

Bader charge	Co	N	C
Co-N_4	-0.9023	4.5102	-3.6076
Co-N_4-C5	-0.9038	4.4839	-3.58

Notes: A positive value indicates the gain of electrons, while a negative value indicates the loss of electrons.

References

[1] G. Kresse, J. Hafner, Phys. Rev. B., 1993, **47**, 558-561.

[2] G. Kresse, J. Hafner, Phys. Rev. B., 1994, **49**, 14251-14269.

[3] K.B. J. P. Perdew, M. Ernzerhof, Phys. Rev. Lett., 1996, **77**, 3865-3868.

[4] G. Kresse, D. Joubert, Phys. Rev. B., 1999, 59, 1758-1775.

[5] S. Grimme, J. Antony, S. Ehrlich, H. Krieg, J. Chem. Phys., 2010, **132**, 3382344.